Experimental and numerical investigation of a micro-ORC system for heat recovery from data centers

Experimental and numerical investigation of a micro-ORC system for heat recovery from data centers

M A Ancona, M Bianchi, L Branchini, A De Pascale, F Melino, S Ottaviano*, A Peretto and C Poletto

Department of Industrial Engineering (DIN) – University of Bologna,
Viale del Risorgimento 2, 40136 Bologna, Italy

saverio.ottaviano2@unibo.it

Abstract. In the effort to enhance the recovery of waste energy, data centers are drawing attention because of the huge amount of heat discharged from the computer racks. Organic Rankine cycle (ORC) power systems are a viable solution to exploit servers' waste heat, as it is available at very low temperatures. The purpose of this study is to assess the feasibility of integrating a micro-ORC system into data centers cooling systems and its potential energy saving. An experimental analysis is carried out on a kW-scale ORC test bench, with R134a as working fluid. Heat is supplied at temperatures and flow rates in the range respectively 40-55 °C and 1.8-5 m³/h, consistently with typical values observed in data centers application, showing the second law efficiency varying between 5% and 13%. Furthermore, a steady-state model of the micro-ORC has been recalibrated and validated against experimental data; the built-in volume ratio of the reciprocating piston expander has been optimized to improve the filling performance of the machine. A parametric analysis, varying the boundary conditions within their range of interest for this application, and the working fluid (R1234yf and R1234ze(E)), shows that a maximum second law efficiency of 30% is achievable with R1234ze(E).

1. Introduction

In the last few decades, data centers have gained a role of primary importance in the information and communication technology field, as they represent a key infrastructure for services provided via the Internet. Their function is not only limited to data storage, but also includes other services related to the processing and the management of digital data, and the virtual exchange of information [1]. From a structural point of view, data centers may be described as large containers inside which they host organized rows of racks, in which modular elements are housed [2].

A critical issue related to data centers is the great amount of energy supply they need: according to Koomey (2005) [3], servers require more than 1.2% of the total U.S. energy consumption and around 0.8% of worldwide use. Cho et al. [4] write about an increasing rate of 20% of data center energy consumption per year, because of an annual increase of 13% of servers and 56% of the data storage demand. Based on more recent statistics, in 2017 data centers energy demand has reached 416.2 billion kWh of electricity, which is almost 2% of the world's total electricity consumption [5], and about 2% of the total greenhouse gas emission [6] (respectively 3% and 4% in the industry field [7]).

The issue of the high energy intensity of data centers is also due to the conversion of 99% of their power into heat, the 70% of which needs to be completely removed, in order to grant safe and reliable operation [2][4]. According to Ebrahimi et al. [8], a rack with a 0.65 m² footprint requires to dissipate

30 kW of thermal power, but it can increase up to 60 kW in case of supercomputer servers filling the rack [9].

In the light of the above, many studies available in literature focus on data centers cooling technologies and low-grade waste heat recovery systems. Nadjahi et al. [9] deeply investigated different kinds of data centers cooling technologies: in particular, free cooling, liquid cooling, two-phase technologies, and building envelope are discussed and compared. Ljungdahl et al. [10] developed a decision supported model to prove potential energy performance efficiencies when liquid cooling and latent thermal energy storage substitute air-based cooling system (which represent more than 90% of the overall data center industry [11]) in data center and high-performance computing cluster. Orò et al. [12] confirmed the reduction of the overall data center consumption by up to 30%, and they applied the liquid cooling configuration to a case study of a swimming pool. Zhang et al. [13] built an economic evaluation model to encourage the development of the data center waste heat recovery in China. Yu et al. [14] carried out a numerical analysis on a case study of a data center in Harbin (China). Deymi-Dashtebayaz and Valipour-Namanlo [15] investigated the technical and economic feasibility of employing an air source heat pump to recover the waste heat, released by a case study data center in Mashahd (Iran), for space heating purposes. Ebrahimi et al. [8] reviewed the low-grade waste heat recovery technologies that may be applied to data centers cooling streams: the Authors outlined that absorption refrigeration [16] and organic Rankine cycle seem to be the most promising and economically feasible technologies for data center waste heat recovery, considering both data centers' working thermodynamic conditions and waste heat recovery techniques' operational requirements. Gupta and Puri [17] provided a technical and economic analysis modelling a hybrid data center infrastructure including water-cooled high-density computing racks and air-cooled low-density server racks. Ding et al. [18] proposed an integrated system of free cooling and heat recovery from data centers, that can work in four different modes (mechanical cooling and mechanical heat recovery, pump free cooling and pump heat recovery), according to cooling conditions and heating demands from staff office: the Authors experimentally proved the feasibility of such an integrated system, especially in northern cold cities. Lin et al. [19] proposed an integrated system to exploit the waste heat of data centers to satisfy the annual demand for heating, cooling and sanitary hot water, by combining a CO2 heat pump with a lithium bromide-water absorption refrigeration system.

The main difficulty associated with reusing data centers' waste energy is that the heat is usually of very low quality, with temperatures lower than 60 °C. Organic Rankine cycle (ORC) technology seems to be a promising solution to exploit low-grade heat sources [20], although thermodynamic intrinsic limits on the electricity production, due to low Carnot efficiency. To the Authors knowledge, just a few studies deal with such an application, especially from an experimental point of view. Ebrahimi et al. [21] numerically investigated the opportunity to integrate an ORC system into a data center cooling system: the Authors developed a steady-state thermodynamic model to assess the cycle performance and a first-order economic analysis, which estimates a payback period in the range 4 - 8 years. Marshall and Duquette [22] proposed a techno-economic analysis of data centers waste heat reuse by heat pump assisted ORC cooling systems. Jawad Al-Tameemi et al. [23] performed a steady-state thermodynamic evaluation on an integrated system aiming at providing cooling for the data center as well as supplying hot water for central heating: the modelled system includes an ORC, a heat pump and a gas burner. An ammonia trilateral Rankine cycle is applied into a stand-alone data center integrated system, simulated by Temiz and Dincer [24], and consisting of a bifacial photo-voltaic power plant, a hydrogen storage system to compensate for the intermittency of the renewable source, and the trilateral Rankine cycle to satisfy the cooling demand and to produce additional electric energy from the waste heat. The same Authors proposed also a system specifically designed for the cooling and electricity needs of data centers [25]: the integrated system includes a parabolic trough-type concentrated solar plant with a Rankine cycle, a bifacial photovoltaic plant, a hydrogen storage system, and a Li-Br absorption refrigeration cycle.

In this context, this study aims to prove the feasibility of recovering very low-grade heat released by servers through ORC technology. An experimental campaign has been carried out with a recuperated

kW-sized ORC test bench: hot source boundary conditions have been replicated consistently with typical values observed in data centers application. Experimental data have been used to recalibrate and validate an already available semi-empirical model of the test bench. In addition, an optimization of the expander built-in volume ratio has been carried out to improve the filling performance of the machine in strongly off-design conditions. Eventually, a parametric analysis with variable boundary conditions and a performance comparison with low-GWP (Global Warming Potential) alternative fluids has been carried out.

2. Methodology

In this section, a description of the micro-ORC test bench adopted to carry out the experimental campaign of this work and the model validation is provided. Then, the approach adopted to model the system is briefly presented.

2.1. Micro-ORC test bench description

The 3 kW-size recuperated ORC test rig, installed at the University of Bologna, has been conceived to exploit low-temperature heat sources (below 100°C). It is composed of three circuits (Figure 1): the internal ORC circuit and two water external circuits, namely the heat source and the cooling system.

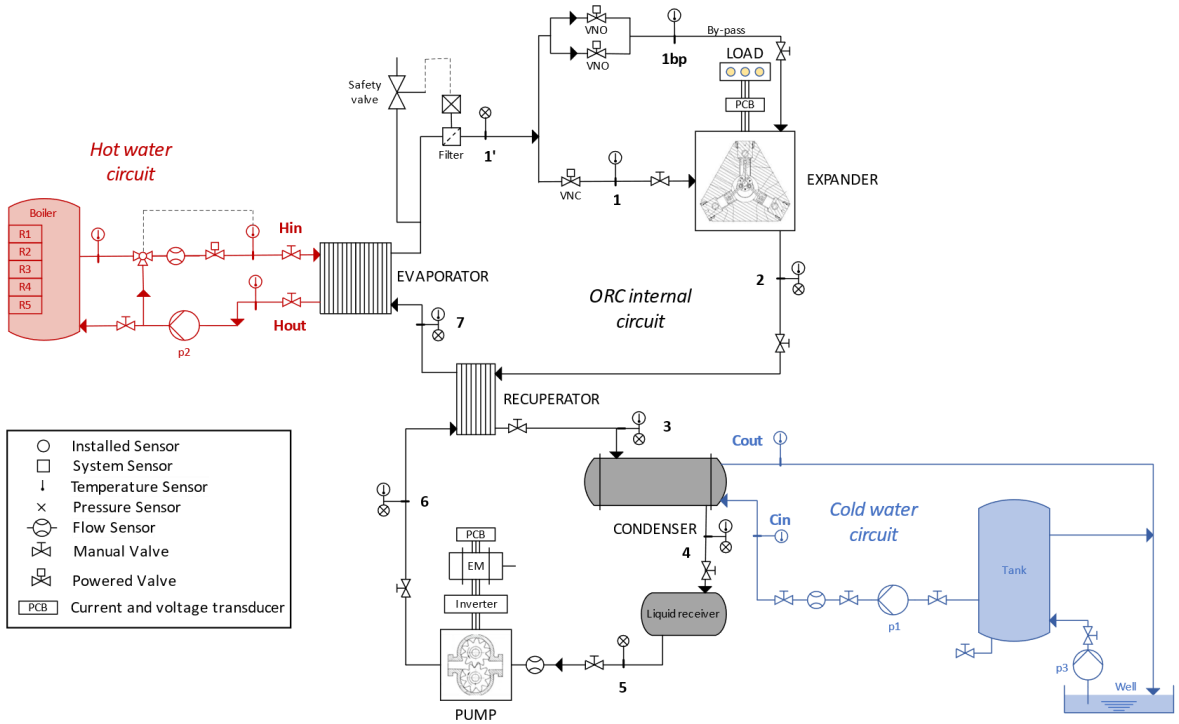

Figure 1. Micro-ORC test bench layout

The internal ORC circuit, operating with HFC-134a as working fluid, involves seven main components: (i) a reciprocating pistons expander, a prototype designed and developed by StarEngine Company, made of three radial cylinders, placed at 120°, for a total displacement of 230 cm³ (more information is available on the patent document [26]); (ii) an external gear pump, driven by a three-phase motor by means of an inverter; (iii) the electrical load, connected to the generator and made of five parallel pure resistive loads of 600 W each (for a maximum of 3000 W); two brazed plate heat exchangers, namely (iv) the evaporator, consisting of 64 plates, and (v) the recuperator, made of 19 plates; (vi) a shell and tube condenser, and (vii) a 19-l tank liquid receiver.

In the hot source circuit, the thermal input is provided by a 500-l electric water boiler, rated for a maximum thermal input of 40 kW; the hot water is circulated by a variable flow centrifugal pump P2. The cooling system is supplied by cold water extracted from a well by pump P3, or coming from the sink, and stored in a 300-l tank, from which water is circulated to the condenser by the centrifugal pump P1.

Several manual valves (VM) are installed all along with the three loops for inspection and in case of breaking; in addition, a normally closed valve (VNC) and two normally open valves (VNO) are installed before the expander to allow the cylinders by-pass during the ORC start-up operation. Moreover, the hot water temperature is adjusted and controlled by a three-way valve, which regulates the fraction of water flow rate recirculating from the outlet of the evaporator and mixing with the hotter flow rate directly coming from the boiler.

The test bench is instrumented with dedicated sensors: temperature and pressure sensors have been located at the inlet and outlet of each component, the working fluid mass flow rate is provided by a Coriolis flow meter, while two magnetic flow meters detect the volumetric flow rate of water feeding the evaporator and the condenser. Two printed circuit boards (PCB), made of voltage and current transducers, have been realized at the laboratory to acquire the electric power produced by the expander generator and the pump motor consumption.

All acquired signals are transmitted to a workstation through a National Instrument CompactRIO device, which includes a FPGA chassis, with a series of FPGA modules for analogue input, and a Real-Time embedded controller. A dedicated real-time data acquisition software has been developed in the LabVIEW environment to process all the acquired measurements and control the valves and the actuators of the system.

2.2. Modelling approach

A thermodynamic steady-state model of the reference micro-ORC power plant, introduced in previous works of the Authors [27] [28] [29], has been readapted in order to investigate the system performance, under variable inputs and with different working fluids. The model is based on a semi-empirical, lumped parameters concept, and has been developed in MATLAB environment with the integration of the open-source library CoolProp [30], for the calculation of the thermodynamic properties of the organic fluid. The model follows a modular approach, in which the ORC main components are modelled separately as MATLAB functions, and linked together at high level to simulate the behavior of the whole cycle. The inputs and outputs of each sub-model are the thermodynamic properties of the working fluid at the inlet and outlet of the corresponding component. Figure 2 shows the framework of the system model, highlighting input and output variables of the whole model and the relationships between the components sub-models. All the empirical parameters of the sub-models have been recalibrated with experimental data, acquired in a test campaign conducted at low heat source temperature (< 60 °C).

2.2.1. Heat exchangers. The heat exchangers (evaporator, recuperator and condenser) are modelled according to a moving boundary approach [31]. In the most general case, the heat transfer surface is divided into three zones, corresponding to the subcooled liquid, two-phase mixture and superheated vapour [32]. The extent of each zone is not fixed but it depends on the heat transfer area needed by the fluid to complete the process related to each specific zone (i.e., in the case of the evaporator, the processes are the heating of the subcooled liquid, the vaporization, and the superheating). The sum of the extensions of all the zones must be equal to the overall heat transfer area, which was determined for each heat exchanger through an empirical procedure, starting from the information available in the datasheets. The heat transfer process occurring in each zone is computed through the ε-NTU (Number of Transfer Units) method. In the subcooling and in the superheating zones of the evaporator and of the condenser, the global heat transfer coefficient is calculated through the Dittus-Boelter correlation for forced convection, while in the two-phase zone and in the single-phase zone of the recuperator, the global heat transfer coefficient derives from empirical correlations [33].

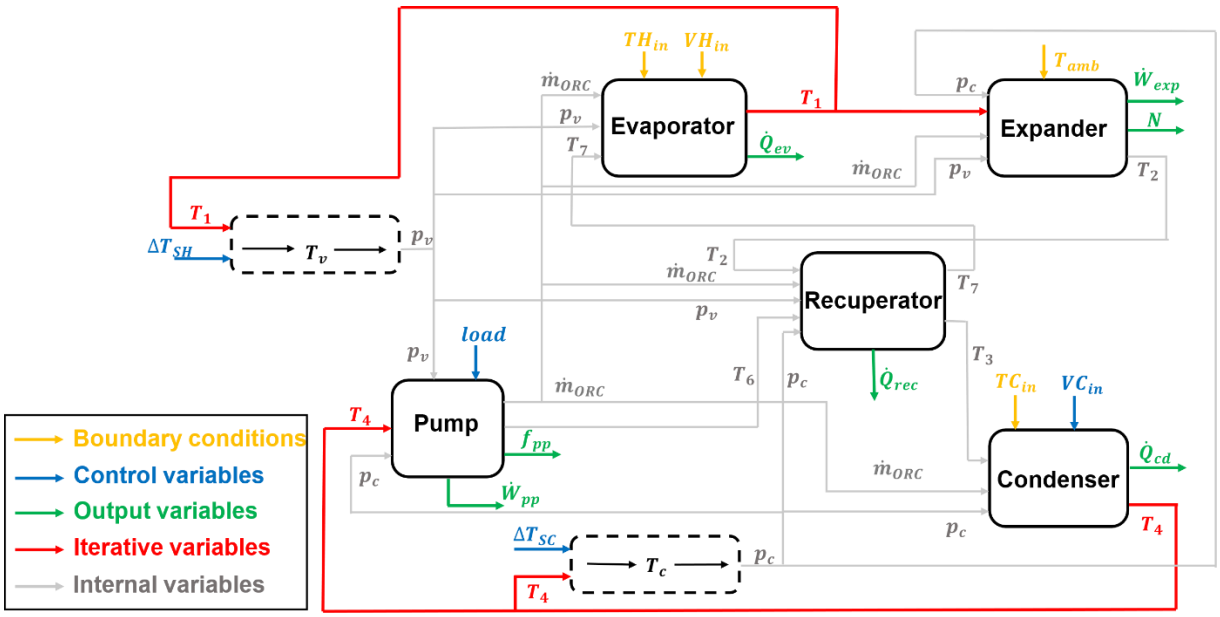

Figure 2. ORC-cycle model block diagram

2.2.2. Pump. In the pump function a system of two equations, describing the characteristic curve of the pump and the resistance curve of the circuit, provides the working fluid flow rate and the pressure rise [28].

2.2.3. Expander. The piston expander model has been described previously in [27][34], and is based on the lumped parameter approach introduced by Glavatskaya in [35]: it reproduces the behavior of the working fluid to obtain the outlet thermodynamic conditions and the output electric power. Figure 3(a) describes the cycle of the working fluid inside the cylinders in the pressure-volume diagram, which involves the fluid admission (1-2), the internal expansion (2-4), the fluid exhaust (4-5) and the re-compression (5-1). The internal expansion (and re-compression) phenomenon is modelled as the sequence of an isentropic expansion (compression) and a constant volume expansion (compression). The output electric power is computed as the ideal thermodynamic expansion power decreased by the several contributions of internal losses, which include leakages, heat dissipation through the expander wall, under and over-expansion losses, frictions and electro-mechanical conversion losses. Losses due to under-expansion and over-expansion take place when the pressure at the end of the isentropic expansion process is greater and lower, respectively, than the discharge pressure (Figure 3(b)(c)).

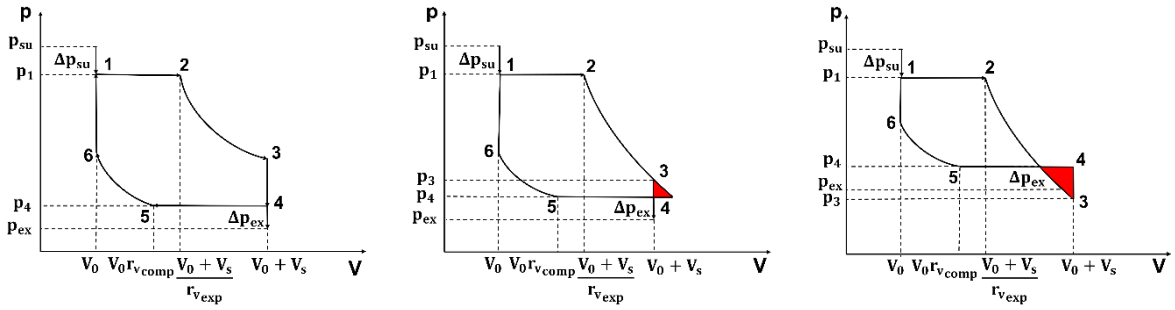

(a) (b) (c)

Figure 3. Expander model p-V diagram (a), in case of under-expansion (b) and over-expansion (c)

The pressure at the end of the isentropic expansion depends on intake stroke ratio, α, which represents the relative volume swept by the piston between the open and the closure of the admission valve, V_2, and it is equal to the inverse of the built-in volume ratio, $r_{v_{exp}}$ (Eq. (1)):

$$\alpha = \frac{V_2}{V_0 + V_s} = \frac{1}{r_{v_{exp}}} \quad (1)$$

where V_0 is the clearance volume, and V_s is the displacement. Adjusting the value of α, for example through a variable valve timing (VVT) system, it is possible to match the internal volumetric expansion ratio with the internal pressure ratio ($p_3 = p_4$).

In this work, a numerical procedure to optimize the expander built-in volume ratio for each tested condition has been implemented, in order to improve the expander design to enhance the filling efficiency. In a previous work [27], the Authors already proved the substantial improvement of the expander performance due to the optimization of the built-in volume ratio.

2.2.4. Fluid dependent parameters correction. Among all the experimental parameters, global heat transfer coefficients are not dependent on the component geometry, but they are associated with the working fluid: therefore, they are corrected according to Giuffrida's procedure [36] to account for different simulated working fluids.

2.3. Performance indexes

Variables analysed to evaluate the feasibility of recovering very low-grade waste heat through a micro-ORC are the following: i) the thermal power input, which provides an idea of the order of magnitude of servers size necessary to the application of such a system; ii) the expander output power and iii) the net power production, which are the electric power produced by the ORC, respectively gross and net of the pump consumption; iv) the net efficiency, which is the ratio of the net power production and the thermal power input, and v) the overall efficiency, which is presented in the form of a second law efficiency, η_{II}, defined as the net system efficiency, η_{net}, over the Carnot efficiency, η_{Carnot}:

$$\eta_{II} = \frac{\eta_{net}}{\eta_{Carnot}} = \frac{\dot{W}_{exp} - \dot{W}_{pp}}{\dot{Q}_{ev}} \cdot \frac{1}{\eta_{Carnot}} \quad (2)$$

where $\dot{W}_{exp}$ and $\dot{W}_{pp}$ are respectively the expander electric power output and the pump electric consumption, while $\dot{Q}_{ev}$ is the thermal power input in the evaporator.

3. Results and Discussion

In this section, the experimental results are presented, followed by the numerical estimations.

3.1. Experimental results

The first aim of the experimental campaign was to assess the operability of the reference micro-ORC test bench under strongly off-design conditions, which are characteristic of data centers application. The experimental test conditions are summarized in Table 1.

Figure 4 shows the thermal power input transferred in the evaporator during each of the tested conditions: an almost linear dependency of the thermal power input from the ORC mass flow rate is observed. At lower hot source temperatures, the ORC mass flow rate is limited by minimum pinch point constraint and a minimum superheating degree at the outlet of the evaporator (a further increase of the ORC mass flow rate would lead to an incomplete evaporation).

Table 1. Experimental test conditions

Hot source temperature	40 – 55 °C	Varied
Hot source flow rate	2 – 5 m³/h	
Cold sink temperature	16 °C	Constant
Cold sink flow rate	7 m³/h	

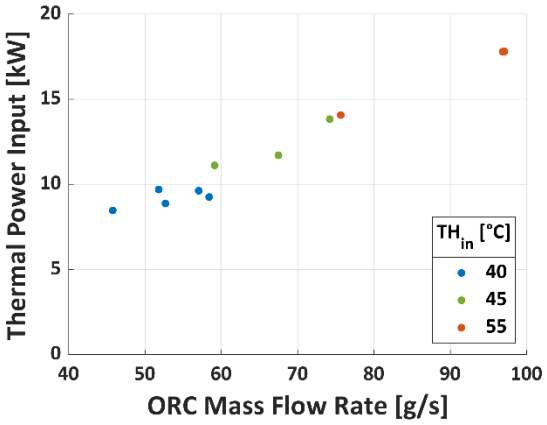

Figure 4. Thermal power input in experimental tests

The experimental campaign proves the system operation feasibility also in very off-design working conditions, indeed an electric power production has been resulted. The expander electric power output, $\dot{W}_{exp}$, (Figure 5) increases with both the ORC mass flow rate and hot source temperature, from a minimum close to 200 W at TH_{in} = 40 °C, and a maximum close to 550 W at TH_{in} = 50 °C.

The Carnot efficiency, η_{Carnot}, due to the low temperature difference between heat source and cold sink, results around 10% in the tested conditions. The value of the second law efficiency, η_{II}, varies between 5% and 13% (Figure 6), increasing with the ORC mass flow rate and the hot source temperature.

Despite the low performance, the experimental campaign proves the feasibility of the application of the ORC technology to recover waste heat from data centers. Furthermore, as the reference system is not designed for this specific application, there is still high room for improvement.

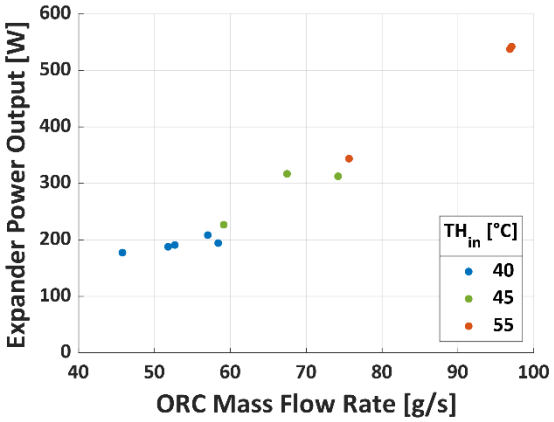

Figure 5. Expander electric power output in experimental tests

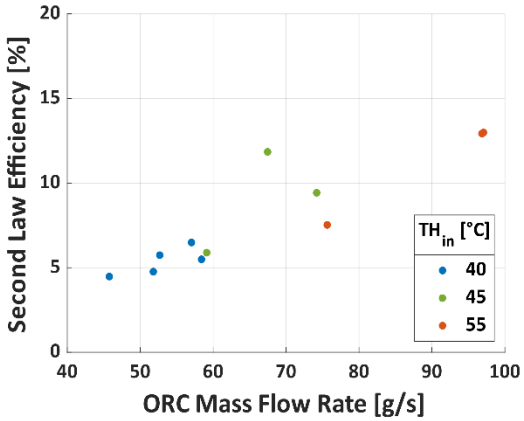

Figure 6. Second law efficiency in experimental tests

3.2. Numerical analysis

The experimental data have been used to recalibrate and validate the semi-empirical model of the reference micro-ORC system for the application with very low hot source temperatures (Figure 7, Figure 8).

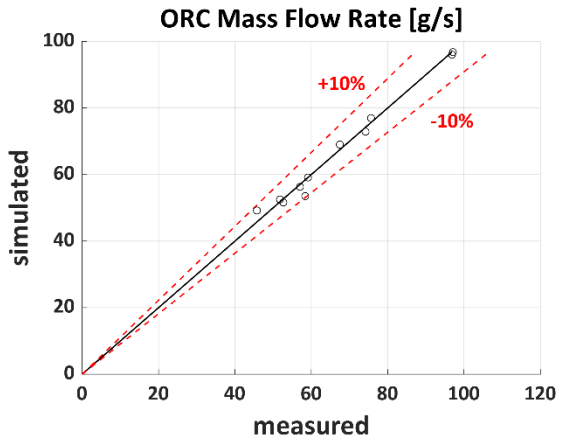

Figure 7. ORC mass flow rate parity plot

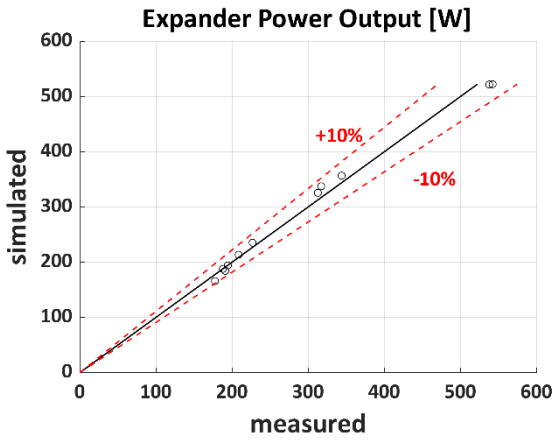

Figure 8. Expander electric power output parity plot

3.3. Optimization of the built-in volume ratio

Implementing an optimization procedure of the expander built-in volume ratio, $r_{v_{exp}}$, allows to carry out a comparison of the performances obtainable with different working fluids. Figure 9 reports the results of the procedure, showing that a slight increase in the expander power output and isentropic efficiency can be obtained by optimizing the value of $r_{v_{exp}}$.The improvement is more evident with the increment of the ORC mass flow rate, which is proportional to the expander speed: at higher speed, the filling process becomes less efficient, so the regulation of the built-in volume ratio has a more evident effect on the performance.

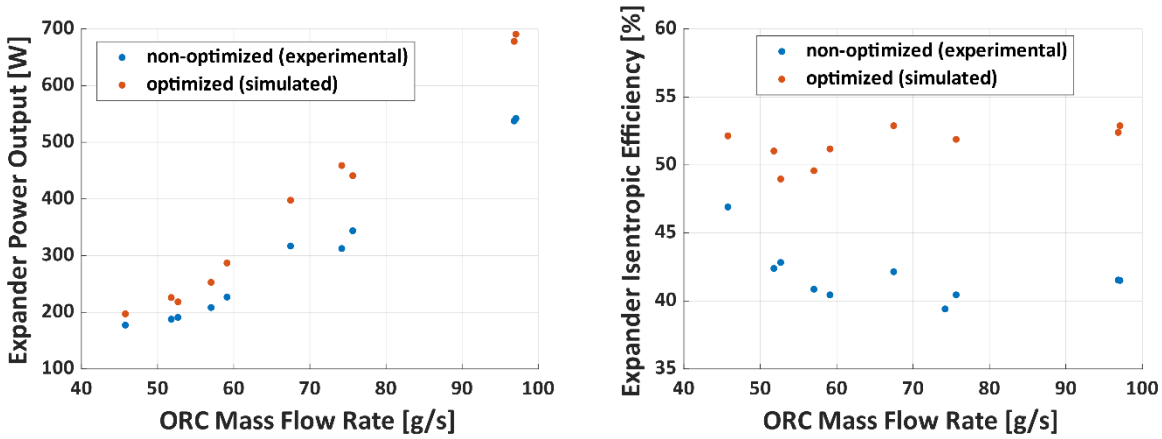

(a) (b)

Figure 9. Expander performance optimization

3.4. Parametric analysis

The optimized model has been used to perform a parametric analysis varying the hot source temperature, TH_{in}, and flow rate, VH, consistently with typical values observed in data centers applications. Furthermore, the investigation has been carried out for three different cold sink temperatures, TC_{in}, to observe how the ambient conditions affect the performance. The input variables adopted in the simulations are listed in Table 2.

Table 2. Parametric analysis input variables

Hot source temperature	40 – 50 °C
Hot source flow rate	0.6 – 1.4 l/s
Superheating degree	3 °C
Cold sink temperature	5 - 25 °C
Cold sink flow rate	2 l/s
Subcooling degree	3 °C
Load	3

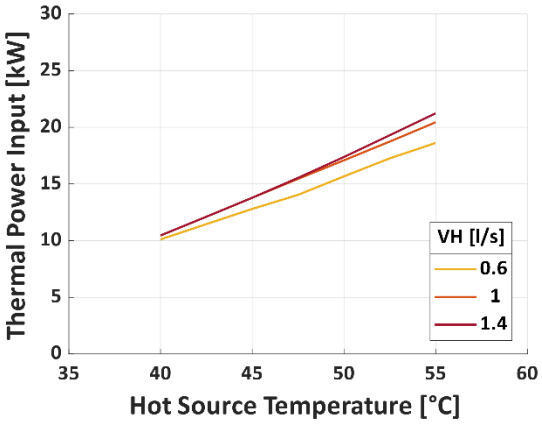

Figure 10. Thermal power input in parametric analysis

Figure 10 shows that the thermal power input depends mainly on the hot source temperature, while the effect of the hot source flow rate, VH, is limited, especially at the lowest values of hot source temperature. The thermal power increases from 10 kW to more than 20 kW as the hot source temperature rises from 40 °C to 55 °C. Reasons lay again in pinch point constraints: an increase of VH results in just a slight decrease of the hot source heat transfer curve slope, which is already almost flat, thus just a slight increase in ORC mass flow rate (and evaporating pressure) is allowed; on the contrary, an increase of the hot source temperature results in the transfer of the hot source heat transfer curve, allowing to increase the ORC mass flow rate (minimum pinch point constraint).

The system performance varies significantly also with the cold sink temperature, TC_{in}. Figure 11 shows the trend of the net power production as function of the hot source temperature, at different values of the cold sink temperature. In the case of maximum hot source temperature (55 °C), the net power production is more than 1 kW with the minimum cold sink temperature (5 °C), while it drops under 300 W with a cold sink temperature of 25 °C. Moreover, for lower hot source temperatures and higher cold sink temperatures, the system is not able to produce net power. The second law efficiency (Figure 12), in the most favourable case, is assessed around 30% with the cold sink temperature equal to 5 °C.

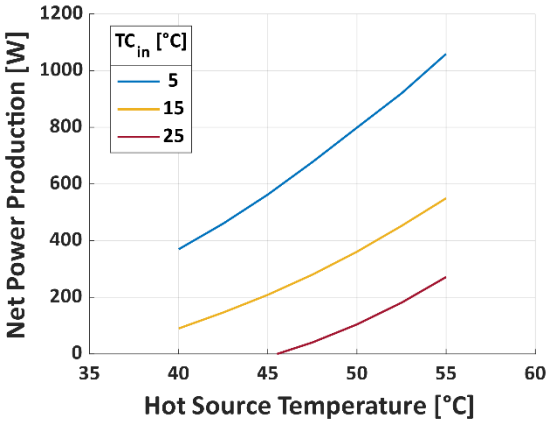

Figure 11. Net electric power output in parametric analysis

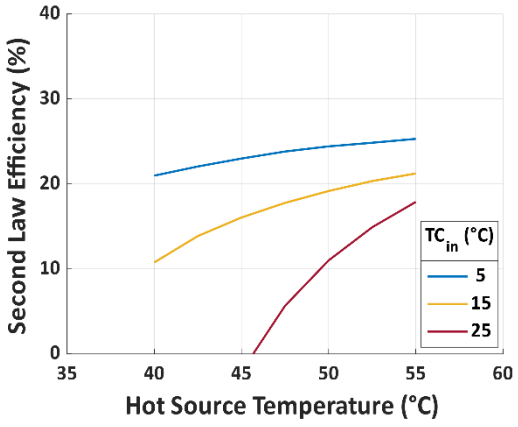

Figure 12. Second law efficiency in parametric analysis

The optimized model has been used to carry out a performance comparison with two low-GWP working fluids, namely R1234yf and R1234ze(E): both these olefins (HFO) are considered viable

alternatives to replace R134a, as they present similar thermodynamic properties, but a substantially lower environmental impact (Table 3).

Table 3. Working fluids selection

Fluid Name	Critical Temperature [°C]	Critical Pressure [bar]	GWP 100 [-]
R134a	101.06	40.593	1430
R1234yf	94.70	33.82	4
R1234ze(E)	109.37	36.36	6

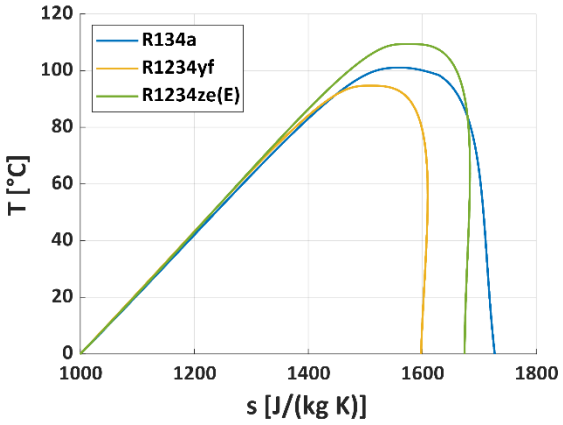

Figure 13. Temperature-entropy diagram of the considered working fluids

The system performances simulated with the low-GWP fluids are comparable with the results obtained with R134a (Figure 14, Figure 15). Considering as reference the most favourable case (cold sink temperature of 5 °C and hot source flow rate of 1.4 l/s), the net output power is slightly higher by using R134a (Figure 14). Concerning the cycle efficiency (Figure 15), instead, R1234ze(E) allows to achieve the maximum net efficiency close to 4.5%, corresponding to a second law efficiency almost equal to 30%, against a value of η_{II} around 27% with R1234yf, and slightly higher than 25% with R134a. The net power production is higher when using R134a since the isentropic enthalpy drop available in the expander is greater: R134a has a higher density and viscosity of the liquid fraction than those presented by the other fluids, therefore it undergoes a lower pressure drop when passing through the expander inlet valve. On the contrary, the cycle efficiency does not show the same trend: reasons lay in the lower thermal power input (Figure 16) introduced in the evaporator with the low-GWP fluids, because of a lower mass flow rate, in the case of R1234ze(E) (Figure 17), and of a lower latent heat of evaporation, in the case of R1234yf (Figure 13). The analysis has been performed at constant values of hot source temperature (50 °C) and superheating degree (3 °C) as described in Table 2, thus the evaporating temperature (and pressure) is determined; similarly, the condensing pressure is imposed by the cold sink temperature and the subcooling degree, equally set for all three fluids. As a result, the ORC mass flow rate, evaluated in the pump model, depends only on the fluid thermodynamic properties, in particular density and viscosity [28]. More in detail, the lower density of R1234ze(E) (also due to the lower operating pressures, resulting from the imposed evaporating and condensing temperatures) results in a lower ORC mass flow rate.

Therefore, considering that about 70% of the power provided to data centers must be removed [2] [4], and thus can be sent as thermal power input to the reference modelled system, R1234ze(E) allows to recover 3% of the electric power required by data centers, followed by R1234yf and R134a, which grants an energy saving of, respectively, 2.8 % and 2.7 %.

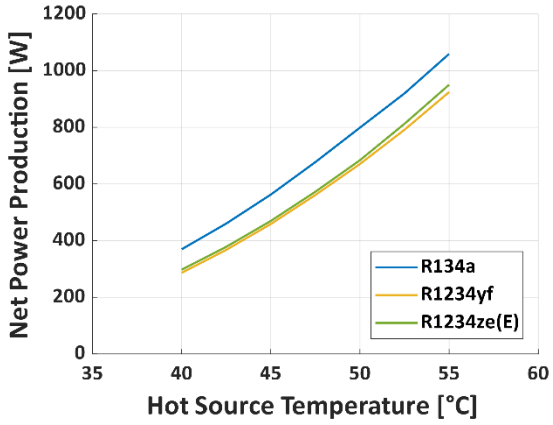

Figure 14. Net electric power output for different working fluids

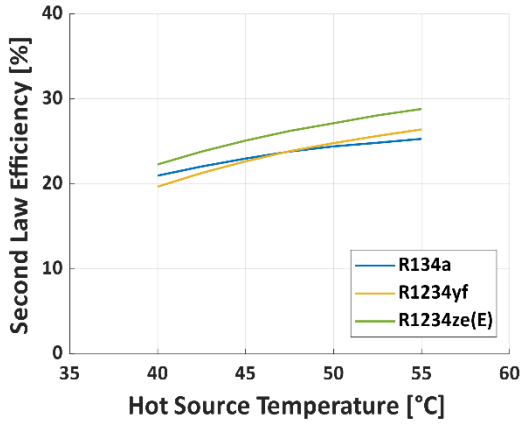

Figure 15. Second law efficiency for different working fluids

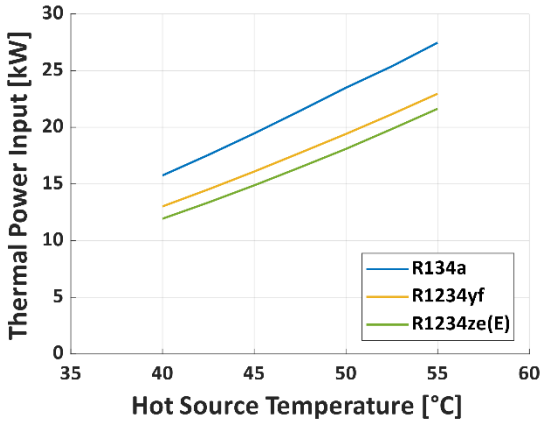

Figure 16. Thermal power input for different working fluids

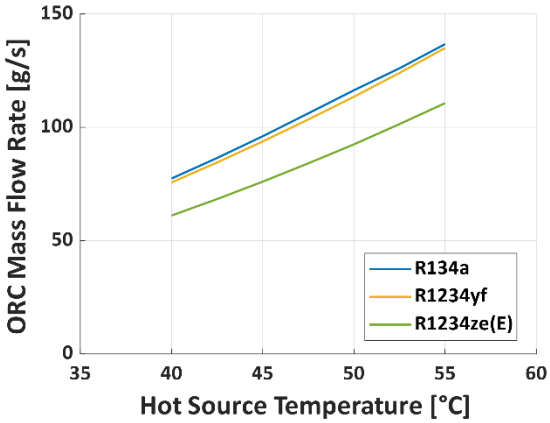

Figure 17. Working fluid mass flow rate

The results of the comparison performed in this study highlight the promising applicability of the two olefins as low environmental impact alternatives to HFC-134a. The optimization of the expander built-in volume ratio allows the comparison to be not affected by the expander filling inefficiencies. Indeed, the procedure improves the system performance with all the three fluids. However, it must be pointed out that, in previous studies [28], [33], [37] [38], the HFOs showed significantly lower performance than R134a, while in this case the performance are comparable. Therefore, the enhancement of the performance, due to the built-in volume ratio optimization, is much more emphasized with low-GWP fluids.

Figure 18 shows the intake stroke ratio, α, which slightly increases with the hot source temperature (and the expander inlet temperature) and with the ORC mass flow rate (Figure 17).

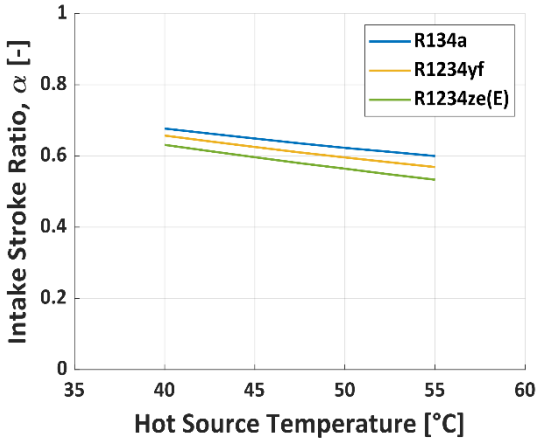

Figure 18. Intake stroke ratio for different working fluids

4. Conclusion

A feasibility analysis of an integrated micro-ORC to recover cooling waste heat from servers is proposed in this work: since data centers are very energy-consuming systems, and almost all the electricity supplied is converted into heat, ORC technology is a viable solution to improve data centers efficiency by reconverting part of the discharged heat into electric energy.

The analysis is carried out with both experimental and numerical investigations: a recuperated kW-sized ORC test bench has been used to prove the feasibility of very low-grade heat recovery, reproducing a heat source with temperatures in the range 40 – 55 °C, consistently with typical values observed in data centers application.

Then a detailed semi-empirical model of the reference micro-ORC has been recalibrated and optimized in the expander built-in volume ratio, to perform a parametric analysis by varying both heat source and ambient conditions: a production of around 1 kW is estimated in the more favourable case, with a net efficiency close to 4.5%. Eventually, a performance comparison changing the reference working fluid (HFC-134a) with low-GWP alternatives (HFO-1234yf and HFO-1234ze(E)) has been carried out: results show comparable performance in terms of power production and second law efficiency with the three considered working fluids: R134a allows to produce the maximum electric power, but with the lowest second law efficiency (25%), whilst R1234ze(E) and R1234yf allow to reach respectively 29 % and 27 %, for an electric power production slightly lower than 1 kW.

As already stated in the introduction, about 70% of the power provided to data centers must be removed: this study proves that recovering the wasted energy allows to save part of the required electric power. Indeed, in terms of electricity savings, R1234ze(E) is the most performing working fluid, as it allows to recover about 3% of the electric power required by data center servers; R1234yf and R134a follow, allowing to recover respectively 2.8% and 2.7% of the electric power consumption. Thus, the numerical analysis assesses the two HFOs to be viable alternatives to the more environmental impacting HFC-134a. Furthermore, it must be pointed out that the reference system, besides including prototypal machines, is not designed for this specific application at very low temperatures, so there is still high room for performance improvement.

4.1. Future developments

A potential future extension of this work would include an investigation of the possibility to replace the water condenser with an air condenser, which would increase the system flexibility and avoid the need for a cooling tower: on the other hand, there would be disadvantages in terms of thermodynamic performance, because of the increment of condensing pressure, and higher auxiliary consumption due to the fan.

Furthermore, the use of the organic fluid to directly cool down the server could be investigated: direct heat transfer would reduce thermal losses and increase the temperature available for heat recovery.

Eventually, partial evaporation could provide a better match between the heat source and WHR system, but it requires special design and optimization study.

Acknowledgements
This work was developed in collaboration with the company 2CRSi Group, which operates in the information technology industry, designing and manufacturing servers for data centers, high performance computers and cloud systems.

References

[1] H. S. Sun and S. E. Lee, 'Case study of data centers' energy performance', *Energy and Buildings*, vol. 38, no. 5, pp. 522–533, May 2006, doi: 10.1016/j.enbuild.2005.08.012.
[2] K. Kant, 'Data center evolution: A tutorial on state of the art, issues, and challenges', *Computer Networks*, vol. 53, no. 17, pp. 2939–2965, Dec. 2009, doi: 10.1016/j.comnet.2009.10.004.
[3] Jonathan G Koomey, 'Estimating Total Power Consumption by Servers in the US and the World', Mar. 2007.
[4] J. Cho, T. Lim, and B. S. Kim, 'Viability of datacenter cooling systems for energy efficiency in temperate or subtropical regions: Case study', *Energy and Buildings*, vol. 55, pp. 189–197, Dec. 2012, doi: 10.1016/j.enbuild.2012.08.012.
[5] Q. Huang, S. Shao, H. Zhang, and C. Tian, 'Development and composition of a data center heat recovery system and evaluation of annual operation performance', *Energy*, vol. 189, no. C, 2019, Accessed: Mar. 16, 2022. [Online]. Available: https://ideas.repec.org/a/eee/energy/v189y2019ics036054421931895x.html
[6] Y. Luo, J. Andresen, H. Clarke, M. Rajendra, and M. Maroto-Valer, 'A framework for waste heat energy recovery within data centre', *Energy Procedia*, vol. 158, pp. 3788–3794, Feb. 2019, doi: 10.1016/j.egypro.2019.01.875.
[7] Y. Luo, J. Andresen, H. Clarke, M. Rajendra, and M. Maroto-Valer, 'A decision support system for waste heat recovery and energy efficiency improvement in data centres', *Applied Energy*, vol. 250, pp. 1217–1224, Sep. 2019, doi: 10.1016/j.apenergy.2019.05.029.
[8] K. Ebrahimi, G. F. Jones, and A. S. Fleischer, 'A review of data center cooling technology, operating conditions and the corresponding low-grade waste heat recovery opportunities', *Renewable and Sustainable Energy Reviews*, vol. 31, pp. 622–638, Mar. 2014, doi: 10.1016/j.rser.2013.12.007.
[9] C. Nadjahi, H. Louahlia, and S. Masson, 'A review of thermal management and innovative cooling strategies for data center', *Sustain. Comput. Informatics Syst.*, 2018, doi: 10.1016/J.SUSCOM.2018.05.002.
[10] V. Ljungdahl, M. Jradi, and C. Veje, 'A decision support model for waste heat recovery systems design in Data Center and High-Performance Computing clusters utilizing liquid cooling and Phase Change Materials', *Applied Thermal Engineering*, vol. 201, p. 117671, Jan. 2022, doi: 10.1016/j.applthermaleng.2021.117671.
[11] E. Oró, P. Taddeo, and J. Salom, 'Waste heat recovery from urban air cooled data centres to increase energy efficiency of district heating networks', *Sustainable Cities and Society*, vol. 45, pp. 522–542, Feb. 2019, doi: 10.1016/j.scs.2018.12.012.
[12] E. Oró, R. Allepuz, I. Martorell, and J. Salom, 'Design and economic analysis of liquid cooled data centres for waste heat recovery: A case study for an indoor swimming pool', *Sustainable Cities and Society*, vol. 36, pp. 185–203, Jan. 2018, doi: 10.1016/j.scs.2017.10.012.
[13] C. Zhang, H. Luo, and Z. Wang, 'An economic analysis of waste heat recovery and utilization in data centers considering environmental benefits', *Sustainable Production and Consumption*, vol. 31, pp. 127–138, May 2022, doi: 10.1016/j.spc.2022.02.006.

[14] J. Yu, Y. Jiang, and Y. Yan, 'A simulation study on heat recovery of data center: A case study in Harbin, China', *Renewable Energy*, vol. 130, pp. 154–173, Jan. 2019, doi: 10.1016/j.renene.2018.06.067.
[15] M. Deymi-Dashtebayaz and S. Valipour-Namanlo, 'Thermoeconomic and environmental feasibility of waste heat recovery of a data center using air source heat pump', *Journal of Cleaner Production*, vol. 219, pp. 117–126, May 2019, doi: 10.1016/j.jclepro.2019.02.061.
[16] K. Ebrahimi, G. F. Jones, and A. S. Fleischer, 'Thermo-economic analysis of steady state waste heat recovery in data centers using absorption refrigeration', *Applied Energy*, vol. 139, pp. 384–397, Feb. 2015, doi: 10.1016/j.apenergy.2014.10.067.
[17] R. Gupta and I. K. Puri, 'Waste heat recovery in a data center with an adsorption chiller: Technical and economic analysis', *Energy Conversion and Management*, vol. 245, p. 114576, Oct. 2021, doi: 10.1016/j.enconman.2021.114576.
[18] J. Ding, H. Zhang, D. Leng, H. Xu, C. Tian, and Z. Zhai, 'Experimental investigation and application analysis on an integrated system of free cooling and heat recovery for data centers', *International Journal of Refrigeration*, Jan. 2022, doi: 10.1016/j.ijrefrig.2022.01.003.
[19] X. Lin, L. Zuo, L. Yin, W. Su, and S. Ou, 'An idea to efficiently recover the waste heat of Data Centers by constructing an integrated system with carbon dioxide heat pump, mechanical subcooling cycle and lithium bromide-water absorption refrigeration cycle', *Energy Conversion and Management*, vol. 256, p. 115398, Mar. 2022, doi: 10.1016/j.enconman.2022.115398.
[20] B.-S. Park, M. Usman, M. Imran, and A. Pesyridis, 'Review of Organic Rankine Cycle experimental data trends', *Energy Conversion and Management*, vol. 173, pp. 679–691, Oct. 2018, doi: 10.1016/j.enconman.2018.07.097.
[21] K. Ebrahimi, G. F. Jones, and A. S. Fleischer, 'The viability of ultra low temperature waste heat recovery using organic Rankine cycle in dual loop data center applications', *Applied Thermal Engineering*, vol. 126, pp. 393–406, Nov. 2017, doi: 10.1016/j.applthermaleng.2017.07.001.
[22] Z. M. Marshall and J. Duquette, 'A techno-economic evaluation of low global warming potential heat pump assisted organic Rankine cycle systems for data center waste heat recovery', *Energy*, vol. 242, p. 122528, Mar. 2022, doi: 10.1016/j.energy.2021.122528.
[23] M. R. Jawad Al-Tameemi, Y. Liang, and Z. Yu, 'Combined ORC-HP thermodynamic cycles for DC cooling and waste heat recovery for central heating', *Energy Procedia*, vol. 158, pp. 2046–2051, Feb. 2019, doi: 10.1016/j.egypro.2019.01.471.
[24] M. Temiz and I. Dincer, 'A unique bifacial PV and hydrogen-based cleaner energy system with heat recovery for data centers', *Applied Thermal Engineering*, vol. 206, p. 118102, Apr. 2022, doi: 10.1016/j.applthermaleng.2022.118102.
[25] M. Temiz and I. Dincer, 'A newly developed solar-based cogeneration system with energy storage and heat recovery for sustainable data centers: Energy and exergy analyses', *Sustainable Energy Technologies and Assessments*, vol. 52, p. 102145, Aug. 2022, doi: 10.1016/j.seta.2022.102145.
[26] G. Zampieri, 'CLOSED-CYCLE PLANT', U.S. Patent No. 20,160,032,786.
[27] M. Bianchi *et al.*, 'Replacement of R134a with low-GWP fluids in a kW-size reciprocating piston expander: Performance prediction and design optimization', *Energy*, vol. 206, p. 118174, Sep. 2020, doi: 10.1016/j.energy.2020.118174.
[28] M. Bianchi *et al.*, 'Performance modelling and greenhouse impact assessment of a micro-ORC energy system working with HFCs, low GWP fluids and mixtures', vol. 238, p. 10002, Oct. 2021, doi: 10.1051/e3sconf/202123810002.
[29] M. A. Ancona *et al.*, 'Simulation of a prototypal micro-ORC for residential application when driven by solar source', presented at the 16th Conference on Sustainable Development of Energy, Water and Environment Systems (SDEWES), Dubrovnik, 2021.
[30] I. Bell, J. Wronski, S. Quoilin, and V. Lemort, 'Pure and Pseudo-pure Fluid Thermophysical Property Evaluation and the Open-Source Thermophysical Property Library CoolProp', *Industrial and Engineering Chemistry Research*, vol. 53, 2014, doi: 10.1021/ie4033999.

[31] D. Ziviani *et al.*, 'Development and a Validation of a Charge Sensitive Organic Rankine Cycle (ORC) Simulation Tool', *Energies*, vol. 9, no. 6, Art. no. 6, Jun. 2016, doi: 10.3390/en9060389.
[32] R. Dickes, O. Dumont, L. Guillaume, S. Quoilin, and V. Lemort, 'Charge-sensitive modelling of organic Rankine cycle power systems for off-design performance simulation', *Applied Energy*, vol. 212, pp. 1262–1281, Feb. 2018, doi: 10.1016/j.apenergy.2018.01.004.
[33] M. A. Ancona *et al.*, 'Solar driven micro-ORC system assessment for residential application', *Renewable Energy*, vol. 195, pp. 167–181, Aug. 2022, doi: 10.1016/j.renene.2022.06.007.
[34] M. Bianchi *et al.*, 'Application and comparison of semi-empirical models for performance prediction of a kW-size reciprocating piston expander', *Applied Energy*, vol. 249, pp. 143–156, Sep. 2019, doi: 10.1016/j.apenergy.2019.04.070.
[35] Y. Glavatskaya, P. Podevin, V. Lemort, O. Shonda, and G. Descombes, 'Reciprocating Expander for an Exhaust Heat Recovery Rankine Cycle for a Passenger Car Application', *Energies*, vol. 5, no. 6, Art. no. 6, Jun. 2012, doi: 10.3390/en5061751.
[36] A. Giuffrida, 'Modelling the performance of a scroll expander for small organic Rankine cycles when changing the working fluid', *Applied Thermal Engineering*, vol. 70, no. 1, pp. 1040–1049, Sep. 2014, doi: 10.1016/j.applthermaleng.2014.06.004.
[37] M. Bianchi *et al.*, 'Performance and total warming impact assessment of pure fluids and mixtures replacing HFCs in micro-ORC energy systems', *Applied Thermal Engineering*, vol. 203, p. 117888, Feb. 2022, doi: 10.1016/j.applthermaleng.2021.117888.
[38] C. M. Invernizzi, P. Iora, M. Preißinger, and G. Manzolini, 'HFOs as substitute for R-134a as working fluids in ORC power plants: A thermodynamic assessment and thermal stability analysis', *Applied Thermal Engineering*, vol. 103, pp. 790–797, Jun. 2016, doi: 10.1016/j.applthermaleng.2016.04.101.